Fabrication of oriented $L1_0$-FeCuPd and composite bcc-Fe/$L1_0$-FeCuPd nanoparticles: Alloy composition dependence of magnetic properties

Hiroshi Naganuma,[a] Kazuhisa Sato, and Yoshihiko Hirotsu
The Institute of Scientific and Industrial Research, Osaka University, 8-1 Mihogaoka, Ibaraki, Osaka 567-0047, Japan

(Presented on 2 November 2005; published online 20 April 2006)

Oriented and well-isolated $L1_0$-FeCuPd ternary alloy nanoparticles have been fabricated by electron-beam evaporation followed by postdeposition annealing. A single $L1_0$ phase was formed in the FeCuPd nanoparticles with (Fe+Cu) content lower than 48 at. %. A strong preferential *c*-axis orientation along the film normal direction was achieved by Cu addition, which leads to a strong perpendicular magnetic anisotropy. Also, a lowering of the ordering temperature by 50 K compared to the binary $L1_0$-FePd nanoparticles was achieved by Cu addition. By contrast, composite particles composed of the bcc Fe and the $L1_0$-FeCuPd were formed when the (Fe+Cu) content was higher than 52 at. %. Coexistence of the bcc Fe and the $L1_0$-FeCuPd was confirmed by high-resolution transmission electron microscopy and nanobeam electron diffraction. It was found that perpendicular magnetic anisotropy of the $L1_0$-FeCuPd nanoparticles on the NaCl substrate is sensitive to the alloy composition. © *2006 American Institute of Physics*.
[DOI: 10.1063/1.2165604]

I. INTRODUCTION

The assembly of the isolated $L1_0$-ordered FePt or FePd nanoparticles has attracted much interest as one of the candidate for future high-density magnetic recording media because of their high uniaxial magnetic anisotropy energy.[1] However, a high-temperature heat treatment at temperatures around 873 K is necessary to obtain the highly ordered $L1_0$ phase of nanoparticles with high coercivity. One of the current issues of these $L1_0$ materials is the addition of third elements in order to reduce the annealing temperature. In the case of FePt thin films, Cu is well known as one of the most effective elements for reducing the ordering temperature.[2] On the contrary, there have been few reports on the $L1_0$-FePd thin films or nanoparticles with Cu additives so far. Quite recently, we found that the perpendicular magnetic anisotropy was enhanced by addition of Cu to FePd nanoparticles.[3] The origin of the appearance of such a perpendicular anisotropy has not been revealed so far. It is considered that the magnetic properties of the $L1_0$-FeCuPd nanoparticles are sensitive to the alloy composition as well as the Cu site in the ternary $L1_0$ phase. However, the alloy composition dependence of the magnetic properties of the FeCuPd nanoparticles is still an open question.

The present study aims at the synthesis and the characterization of $L1_0$-FeCuPd nanoparticles with different Fe content by transmission electron microscopy and electron diffraction. The nanostructure and magnetic properties were studied as a function of the alloy composition.

II. EXPERIMENTAL PROCEDURE

FeCuPd nanoparticles were fabricated by successive deposition[4] of Pd, Cu, and Fe using an electron-beam evaporation technique onto NaCl (001) substrates kept at 673 K. After the deposition of Fe, an amorphous Al_2O_3 thin film was further deposited to protect the particles from oxidation. Annealing of these specimens for the formation of the $L1_0$-ordered nanoparticles was made in a high-vacuum furnace at 823 K for 3.6 ks. Compositional analyses of these specimens were performed by energy-dispersive x-ray spectroscopy (EDS) attached to a transmission electron microscope (TEM) operated at 300 kV (JEM-3000F). The alloy compositions were changed by adjusting the nominal thickness of each element. The fabricated specimens had Fe content between 36 and 55 at. % with a fixed Cu content of about 7 at. %, namely, $Fe_xCu_7Pd_{93-x}(36 \leqslant x \leqslant 55)$. The nanostructure and morphology of the FeCuPd nanoparticles were characterized by TEM, selected area electron diffraction (SAED), and nanobeam electron diffraction (NBD). The magnetic properties were measured by a superconducting quantum interference device (SQUID) magnetometer.

III. RESULTS AND DISCUSSION

A. Alloy composition dependence of the magnetic properties

Figure 1 shows the (Fe+Cu) concentration dependence of the coercivity for the $Fe_xCu_7Pd_{93-x}$ nanoparticles after annealing at 823 K for 3.6 ks. High perpendicular coercivity values of more than 3 kOe were obtained for the specimen with the (Fe+Cu) content between 43 and 48 at. %. In this composition range, the coercivity values for the in-plane direction were much lower than those of the perpendicular ones, indicating the enhancement of the strong perpendicular magnetic anisotropy. The annealing temperature necessary for obtaining a coercivity higher than 3 kOe was 50 K lower than that of the binary $L1_0$-FePd nanoparticles. Dissolution of Cu into Pd leads to a decrease of the melting temperature,[5]

[a]Electronic mail: hirosi22@sanken.osaka-u.ac.jp

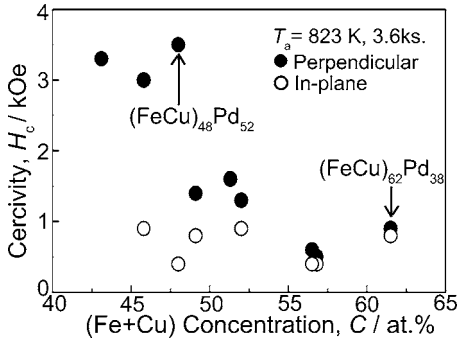

FIG. 1. (Fe+Cu) concentration dependence of the coercivity for the $Fe_xCu_7Pd_{93-x}$ nanoparticles measured at 300 K after annealing at 823 K for 3.6 ks with the external field both perpendicular (solid circles) and parallel (open circles) to the film plane.

which will results in an enhancement of the chemical diffusion constant (D) since the D value is inversely proportional to the melting temperature of the material. By contrast, the coercivity in the perpendicular direction abruptly decreased to the same level as the in-plane coercivity at the (Fe+Cu) content of 49 at. %.

Figure 2 shows the magnetization curves of the $(FeCu)_{48}Pd_{52}$ and the $(FeCu)_{62}Pd_{38}$ nanoparticles measured at 300 K (a) and 10 K (b), respectively. The magnetic field was applied perpendicular to the film plane. The coercivity and the remanence of the $(FeCu)_{48}Pd_{52}$ nanoparticles were higher than those of the $(FeCu)_{62}Pd_{38}$ nanoparticles. At 10 K, coercivities were almost two times higher than those at 300 K for both specimens, indicating the suppression of thermal agitation as well as the increase of the magnetic anisotropy energy at low temperature.

B. Alloy composition dependence of nanostructure

Figures 3(a) and 3(b) show the SAED patterns, the high-resolution TEM (HRTEM) images, and the bright-field TEM images for the $(FeCu)_{48}Pd_{52}$ and the $(FeCu)_{62}Pd_{38}$ nanoparticles after annealing at 823 K for 3.6 ks, respectively. In the SAED pattern shown in Fig. 3(a), superlattice reflections from the $L1_0$-type ordered structure are visible. Many

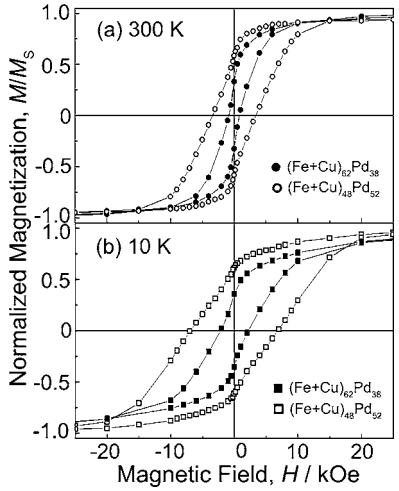

FIG. 2. Magnetization curves of the $(FeCu)_{48}Pd_{52}$ and the $(FeCu)_{62}Pd_{38}$ nanoparticles measured at 300 K (a) and 10 K (b), respectively.

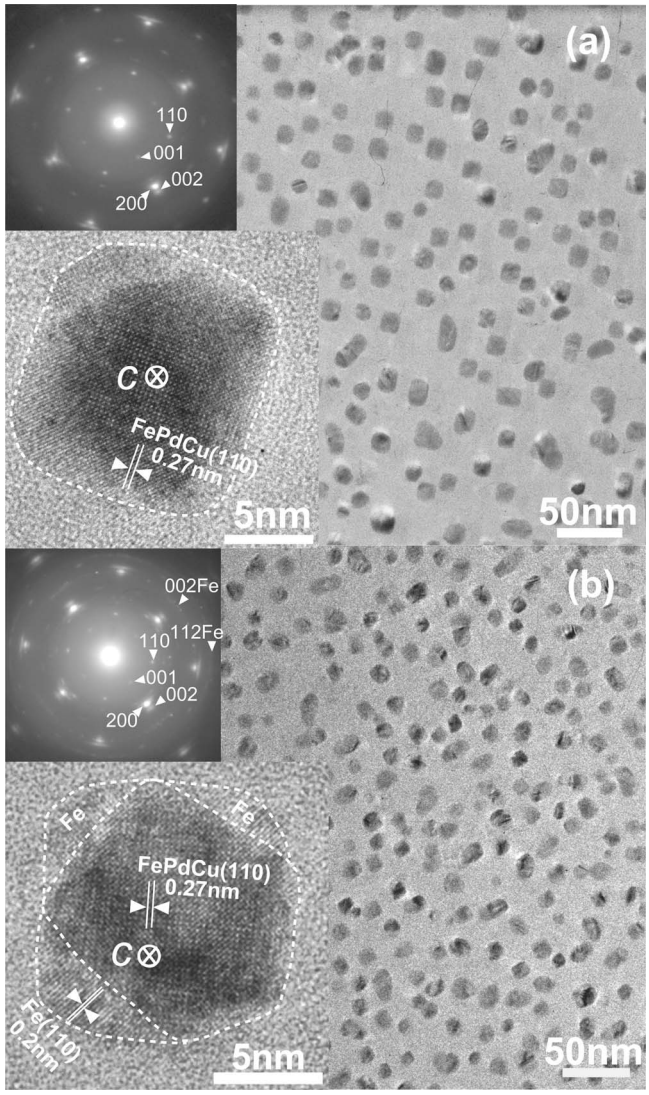

FIG. 3. SAED patterns, HRTEM images, and bright-field TEM images for the $(FeCu)_{48}Pd_{52}$ nanoparticles (a) and the $(FeCu)_{62}Pd_{38}$ nanoparticles (b) after annealing at 823 K for 3.6 ks.

$L1_0$-FeCuPd nanoparticles have a squarelike shape with {110} facets with a preferential c-axis perpendicular orientation showing strong 110 superlattice reflections in the SAED pattern. Actually, this specimen showed a strong perpendicular anisotropy as shown in Fig. 1. By contrast, in the case of the $(FeCu)_{62}Pd_{38}$ nanoparticles, not only the superlattice reflections but also the reflections from the bcc Fe can be seen in the SAED pattern [Fig. 3(b)]. The HRTEM image in Fig. 3(b) shows two types of lattice fringes in the same nanoparticle corresponding to the $L1_0$-FeCuPd and the bcc Fe. The formation of the nanocomposite particles was also confirmed by NBD as shown in Fig. 4. These NBD patterns correspond to local regions in a nanoparticle with the bcc Fe (a) and the $L1_0$-FeCuPd (b) with the c axis oriented perpendicular to the film planes. These results indicate a formation of nanocomposite particles composed of the bcc-Fe and the $L1_0$-FeCuPd phases. The average lattice parameters and the axial ratios are shown in Fig. 5. The axial ratios for the present FeCuPd nanoparticles are in the range between 0.923 and 0.928 and are much smaller than that of the binary $L1_0$-FePd

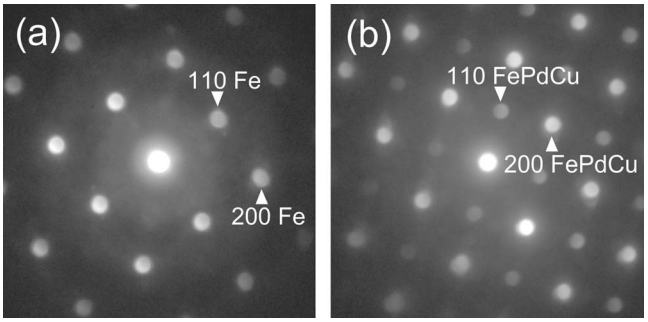

FIG. 4. NBD patterns for the $(FeCu)_{62}Pd_{38}$ nanoparticles after annealing at 823 K for 3.6 ks. The NBD patterns correspond to the local regions in the nanoparticles with bcc Fe (a) and the $L1_0$-FeCuPd of the c axis oriented perpendicular to the film plane (b).

nanoparticles ($c/a=0.959\pm0.004$) (Ref. 4) and close to the value reported in the $L1_0$-$FeCuPt_2$ compound ($c/a=0.923\pm0.001$).[6] The composition of each nanoparticle was independent of the particle size, and also the alloy composition distribution was small ($\sigma\sim2$ at. %) according to the nanobeam EDS analysis. Although, the additive Cu is thought to be responsible for the observed smaller axial ratio, the role of Cu for reducing the axial ratio is still an open question. It should be noted that the lattice parameter and the axial ratio are independent of the alloy composition, indicating the fact that the degree of order is independent of the existence of bcc Fe in the case of the bcc Fe/$L1_0$-FeCuPd, although the coercivity of the nanocomposite particles was lower than that of the $L1_0$-FeCuPd nanoparticles. The observed disappearance of the strong perpendicular magnetic anisotropy in the nanocomposite particles can be attributed to the existence of bcc Fe with cubic anisotropy.

Figure 6 shows the diffracted beam intensity profiles for the FeCuPd nanoparticles measured along the $[001]^*$ direction in the SAED patterns as a function of the (Fe+Cu) content. The annealing condition was 823 K for 3.6 ks for every specimen. Both 001_{FeCuPd} and weak 200_{Fe} reflections coexisted in the specimens with the (Fe+Cu) compositions of 62, 57, and 52 at. %, while the intensity of the 200_{Fe} reflection decreased at 52 at. % and disappeared at 48 at. %, indicating that the amount of the bcc-Fe phase decreased as the composition reached the equiatomic composition of $(FeCu)_{50}Pd_{50}$ (Ref. 7). It can be considered that the additive Cu replaces the Fe site in the $L1_0$-FeCuPd ternary alloy nanoparticles. In other words, although the substitution on

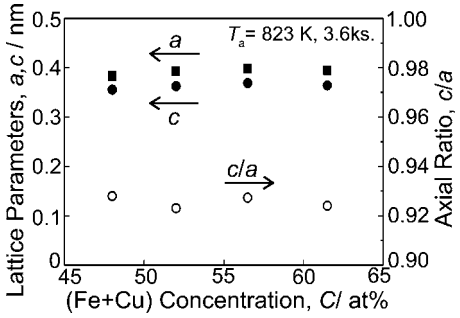

FIG. 5. (Fe+Cu) content dependence of the lattice parameters and the axial ratios for the $L1_0$-FeCuPd nanoparticles. The averaged measurement error was ±0.004 nm for a and c axes and ±0.004 for c/a.

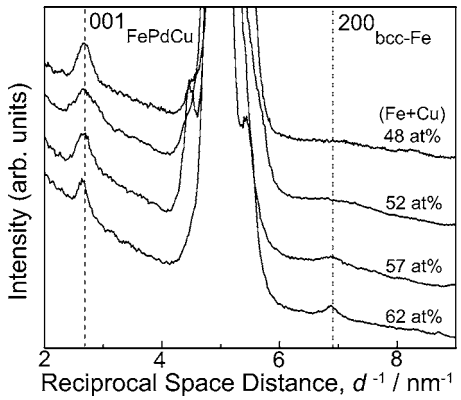

FIG. 6. Diffracted beam intensity profiles for the FeCuPd nanoparticles measured along the $[001]^*$ direction in the SAED patterns as a function of the (Fe+Cu) content.

the Fe site by Cu effectively reduces the ordering temperature, the decrease of Fe atoms will hinder the magnetization when the Cu content becomes larger. The quantitative evaluation of the magnetocrystalline anisotropy constant and the saturation magnetization are necessary for further discussion.

IV. CONCLUSION

$L1_0$-FeCuPd nanoparticles and bcc-Fe/$L1_0$-FeCuPd nanocomposite particles were fabricated by successive deposition of Pd, Cu, and Fe followed by postdeposition annealing at 823 K for 3.6 ks. A high coercivity more than 3 kOe with perpendicular magnetic anisotropy was obtained for the specimens with (Fe+Cu) content between 43 and 48 at. %. The perpendicular coercivity abruptly decreased when the (Fe+Cu) content is higher than 49 at. %. The drastic change of the coercivity is related to the formation of nanocomposite particles composed of bcc Fe and the $L1_0$-FeCuPd. The lattice parameter and the axial ratio were independent of the alloy composition, although the coercivity values of the nanocomposite particles were lower than those of the $L1_0$-FeCuPd nanoparticles. It has been shown that the perpendicular magnetic anisotropy as well as nanostructure can be changed by controlling the alloy composition in the ternary $L1_0$-FeCuPd nanoparticles.

ACKNOWLEDGMENTS

This study was partly supported by the Center of Excellence (COE) program at ISIR, Osaka University and by the Grant-in-Aid for Scientific Research (S) (Grant No. 16106008) from the Ministry of Education, Culture, Sports, Science and Technology, Japan.

[1] D. Weller and M. F. Doerner, Annu. Rev. Mater. Sci. **30**, 611 (2000).
[2] T. Maeda, T. Kai, A. Kikitsu, T. Nagase, and J. Akiyama, Appl. Phys. Lett. **80**, 2147 (2002).
[3] H. Naganuma, K. Sato, and Y. Hirotsu (unpublished).
[4] K. Sato and Y. Hirotsu, J. Appl. Phys. **93**, 6291 (2003).
[5] T. B. Massalski, H. Okamoto, P. R. Subramanian, and L. Kacprzak, *Binary Alloy Phase Diagrams*, 2nd ed. (ASM International, Materials Park, Ohio, 1990), p. 1454.
[6] M. Shahmiri, S. Murphy, and D. J. Vaughan, Miner. Mag. **49**, 547 (1985).
[7] J. Kawamura, K. Sato, and Y. Hirotsu, J. Appl. Phys. **96**, 3906 (2004).